第 33 卷第 4 期
2017 年 4 月

无 机 化 学 学 报
CHINESE JOURNAL OF INORGANIC CHEMISTRY

Vol.33 No.4
692-698

喹啉-8-甲醛缩 4-甲基氨基硫脲 Ni(Ⅱ)/Zn(Ⅱ)/Cd(Ⅱ)/Cu(Ⅱ)配合物的合成、结构和 DNA 结合性质

毛盼东[1] 韩学锋*,[2] 李珊珊[1] 史琳莹[1] 王 元[1] 吴伟娜*,[1]

([1]河南理工大学化学化工学院,焦作 454000)

([2]河南理工大学人事处,焦作 454000)

摘要:合成并通过单晶衍射、元素分析、红外光谱表征了配合物[NiL_2]·2CH_3OH(**1**), [ZnL_2]·CH_3OH(**2**), [CdL_2]·CH_3CH_2OH(**3**)和[$Cu_2L_2Cl_2$](**4**)(HL 为喹啉-8-甲醛缩 4-甲基氨基硫脲)。单晶衍射结果表明,配合物 **1**~**3** 结构相似,中心金属离子与来自 2 个硫醇化脱质子配体 L^-的 4 个 N 原子和 2 个 S 原子配位,采取扭曲的八面体配位构型。而配合物 **4** 中 Cu(Ⅱ)离子与 1 个中性配体 HL 和 3 个氯离子配位,其中 2 个氯离子为 μ^2 桥联。荧光光谱结果表明,所有配合物,尤其是 **4** 与 DNA 的相互作用能力明显强于配体。

关键词:喹啉;缩氨基硫脲;配合物;晶体结构;DNA 相互作用

中图分类号:O614.81+3;O614.24+1;O614.24+2;O614.121 **文献标识码**:A **文章编号**:1001-4861(2017)04-0692-07

DOI:10.11862/CJIC.2017.067

Syntheses, Crystal Structures and DNA-Binding Properties of Ni(Ⅱ)/Zn(Ⅱ)/Cd(Ⅱ)/Cu(Ⅱ) Complexes with 4-Methyl-1-((quinolin-8-yl)methylene)-thiosemicarbazide

MAO Pan-Dong[1] HAN Xue-Feng*,[2] LI Shan-Shan[1] SHI Lin-Ying[1] WANG Yuan[1] WU Wei-Na*,[1]

([1]*College of Chemistry and Chemical Engineering, Henan Polytechnic University, Jiaozuo, Henan* 454000, *China*)

([2]*Personnel Division, Henan Polytechnic University, Jiaozuo, Henan* 454000, *China*)

Abstract: Four complexes [NiL_2]·2CH_3OH (**1**), [ZnL_2]·CH_3OH (**2**), [CdL_2]·CH_3CH_2OH (**3**) and [$Cu_2L_2Cl_2$] (**4**) (HL= 4-methyl-1-((quinolin-8-yl)methylene)-thiosemicarbazide) have been synthesized and structurally determined by single-crystal X-ray diffraction. The results show that the structures of complexes **1**~**3** are quite similar. The metal ion in each complex with a distorted octahedron geometry is surrounded by two anionic thiosemicarbazone ligands with N_4S_2 donor set. However, complex **4** is binuclear, and each central Cu(Ⅱ) ion is coordinated by one independent neutral ligand HL and three chloride anions, two of which act as μ^2-bridges. In addition, the fluorescence spectra indicate that the interactions of the complex es with DNA, particularly of the complex **4**, are stronger than that of the ligand HL. CCDC: 1518183: **1**; 1518184: **2**; 1518185: **3**; 1518186: **4**.

Keywords: quinoline; thiosemicarbazone; complex; crystal structure; DNA interaction

In the past few decades, thiosemicarbazones (TSCs) and their metal complexes have been a focus of chemists and biologists because of their wide range of pharmacological effects, such as antibacterial, antiviral, antifungal, and, most intriguingly, antitumor activity[1]. It is noted that the presence of a heterocyclic ring in the synthesized TSCs plays a major role in extending their pharmacological properties[1]. As a result, the transition metal complexes of TSCs derived from 2-acylpyridine/2-acylpyrazine have been extensively investigated as potential anticancer agents[1-11]. However, the studies on the complexes with TSCs

收稿日期:2016-11-22。收修改稿日期:2017-01-18。

国家自然科学基金(No.21001040)、河南省教育厅自然科学基金(No.12B150011,14B150029)资助项目。

*通信联系人。E-mail:108242720@qq.com; wuwn08@hpu.edu.cn;会员登记号:S06N6704M1112(吴伟娜)。

bearing condensed heterocycles are relatively few [12-14].

On the other hand, the biological activities of TSCs metals depend on not only the structures of the ligands but also the metal centers [6-8]. In most case of TSCs, metal-ligand synergism could occur[1]. Recently, it has been demonstrated that several transition metal complexes with (quinolin-8-yl)methylene)-thiosemicarbazide have been reported to be potential antitumor agents[12-14]. As the continuation of our work on metal-TSCs [14], four transition metal complexes with 4-methyl-1-((quinolin-8-yl)methylene)-thiosemicarbazide (HL, Scheme 1) have been synthesized and structural determined by single-crystal X-ray diffraction. In addition, the interactions between the compounds and ct-DNA have been studied by ethidium bromide (EB) fluorescence probe.

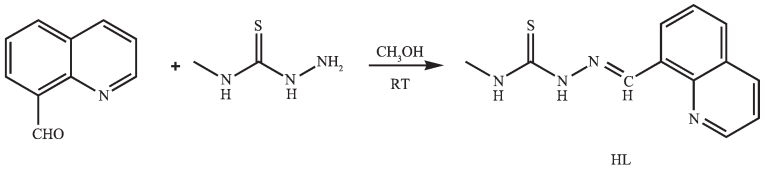

Scheme 1 Synthetic route for the synthesis of HL

1 Experimental

1.1 Materials and measurements

Solvents and starting materials for syntheses were purchased commercially and used as received. Elemental analyses were carried out on an Elemental Vario EL analyzer. ^{1}H NMR spectra of HL was acquired with Bruker AV400 NMR instrument in DMSO-d_6 solution with TMS as internal standard. The IR spectra (ν=4 000~400 cm^{-1}) were determined by the KBr pressed disc method on a Bruker V70 FTIR spectrophotometer. The interactions between the compounds and ct-DNA are measured using literature method [14] via emission spectra on a Varian CARY Eclipse spectrophotometer.

1.2 Preparations of the ligand and complexes 1~4

The TSC ligand HL was produced according to the literature method, while using 4-methylthiosemicabazide instead of thiosemicabazide[13-14]. Anal. Calcd. For $C_{12}H_{12}N_4S$ (%): C: 58.99; H: 4.95; N: 22.93. Found (%): C: 59.12; H: 5.14; N: 22.86. FTIR (cm^{-1}): ν(C=N)1 598, ν(C=N)$_{quinoline}$1 545, ν(C=S) 822. ^{1}H NMR (400 MHz) : δ 11.80 (s, 1H, NH), 9.75~9.77 (q, 1H, NH), 8.95~8.97(1H)/8.47~8.88(2H)/8.09~8.17 (1H)/7.68~7.75(2H) for quinoline-H , 8.22 (s, 1H, CH =N), 3.00~3.04 (d, 3H, CH_3).

The complexes **1**, **2** and **4** were generated by reaction of HL (5 mmol) with equimolar of $Ni(NO_3)_2$, $Zn(NO_3)_2$ and $CuCl_2$ in methanol (10 mL) solution, respectively, while using $Cd(NO_3)_2$ in ethanol (10 mL) solution for the synthesis of complex **3**. Crystals of **1**~**4** suitable for X-ray diffraction analysis were obtained by evaporating the corresponding reaction solutions at room temperature.

1: brown rods. Anal. Calcd. For $C_{26}H_{30}N_8O_2S_2Ni$ (%): C: 51.24; H: 4.96; N: 18.39. Found (%): C: 51.32; H: 5.14; N: 18.26. FTIR (cm^{-1}): ν(C=N)1 570, ν(N=C)$_{quinoline}$1 482, ν(C-S)758.

2: yellow blocks. Anal. Calcd. for $C_{25}H_{26}N_8OS_2Zn$ (%): C: 51.41; H: 4.49; N: 19.19. Found (%): C: 51.33; H: 4.29; N: 19.28. FTIR (cm^{-1}): ν(C=N)1 571, ν(N=C)$_{quinoline}$1 487, ν(C-S)755.

3: yellow blocks. Anal. Calcd. for $C_{26}H_{28}N_8OS_2Cd$ (%): C: 48.41; H: 4.37; N: 17.37. Found (%): C: 48.44; H: 4.29; N: 17.45. FTIR (cm^{-1}): ν (C=N)1 568, ν(N=C)$_{quinoline}$1 495, ν(C-S)759.

4: green blocks. Anal. Calcd. for $C_{24}H_{24}N_8Cl_4S_2Cu_2$ (%): C: 38.05; H: 3.19; N: 14.79. Found (%): C: 38.18; H: 3.29; N: 14.68. FTIR (cm^{-1}): ν(C=N)1 575, ν(N=C)$_{quinoline}$1 502, ν(C=S)780.

1.3.1 X-ray crystallography

The X-ray diffraction measurement for complexes **1**~**4** was performed on a Bruker SMART APEX Ⅱ CCD diffractometer equipped with a graphite monochromatized Mo $K\alpha$ radiation (λ=0.071 073 nm) by using φ-ω scan mode. Semi-empirical absorption correction was applied to the intensity data using the

SADABS program[15]. The structures were solved by direct methods and refined by full matrix least-square on F^2 using the SHELXTL-97 program[16]. All non-hydrogen atoms were refined anisotropically. All H atoms were positioned geometrically and refined using a riding model. SQUEEZE procedure was applied to deal with the existence of the voids of complex **3**. Details of the crystal parameters, data collection and refinements for complexes **1**~**4** are summarized in Table 1.

CCDC: 1518183, **1**; 1518184, **2**; 1518185, **4**; 1518186, **4**.

Table 1 Selected crystallographic data for complexes 1~4

	1	**2**	**3**	**4**
Empirical formula	$C_{26}H_{30}N_8O_2S_2Ni$	$C_{25}H_{26}N_8OS_2Zn$	$C_{26}H_{28}N_8OS_2Cd$	$C_{24}H_{24}N_8Cl_4S_2Cu_2$
Formula weight	609.41	584.03	645.08	757.51
T / K	296(2)	296(2)	296(2)	296(2)
Crystal system	Monoclinic	Monoclinic	Monoclinic	Monoclinic
Space group	$P2_1/c$	$P2_1/c$	$P2_1/c$	$P2_1/c$
a / nm	1.150 27(12)	1.137 7(2)	1.157 52(6)	1.069 9(12)
b / nm	1.231 41(13)	1.222 8(2)	1.233 06(6)	1.641 9(19)
c / nm	1.996 2(2)	1.990 7(3)	2.050 03(10)	0.851 8(9)
β / (°)	94.059(2)	94.136(3)	97.634 0(10)	111.242(17)
V / nm^3	2.820 4(5)	2.762 1(8)	2.900 1(3)	1.395(3)
Z	4	4	4	2
D_c / (g·cm^{-3})	1.435	1.404	1.942	1.804
Unique reflections	4 965	4 870	3 761	2 452
R_{int}	0.054 7	0.059 7	0.038 8	0.029 7
GOF	1.012	1.017	1.026	1.047
R indices [$I>2\sigma(I)$]	R_1=0.042 6	R_1=0.051 4	R_1=0.033 9	R1=0.029 8
	wR_2=0.090 0	wR_2=0.151 3	wR_2=0.071 0	wR_2=0.071 8
R indices (all data)	R_1=0.072 9	R_1=0.075 5	R_1=0.050 9	R_1=0.037 4
	wR_2=0.101 9	wR_2=0.166 2	wR_2=0.075 3	wR_2=0.075 3

2 Results and discussion

2.1 Crystal structures description

The diamond drawings of the asymmetric unit of **1**~**4** are shown in Fig.1. Selected bond distances and angles are listed in Table 2. Hydrogen bonds information is in Table 3. The lengths of C-S bond are in the range of 0.169 0(5) and 0.173 3(5) nm in complexes **1**~**3**, while that in complex **4** being 0.167 5(3) nm. This fact indicates that the ligand HL has thiolated and deprotonated in complexes **1**~**3**[14], whilst acts as neutral ligand in complex **4**.

As shown in Fig.1a ~1c, the structures of complexes **1**~**3** are quite similar, while with different crystal solvent molecules. The metal ion in each complex with a distorted octahedron geometry is surrounded by two anionic TSC ligands with N_4S_2 donor set. The distances of metal-N/S bonds (Table 2) were comparable with those found in the reported complexes with similar donor set[14]. In the crystals of complexes **1** and **3**, intermolecular N-H···N hydrogen bonds link the complex molecules into one-dimentional chains along b axis (Fig.2a and 2c). Furthermore, the intermolecular O-H···N and OH···O hydrogen bonds between the lattice methanol molecules and complex molecules are also present in **1** (Table 3). By contrast, in the crystal of **2**, the intermolecular N-H ··· N, N-H ··· O and O-H ··· N hydrogen bonds link the complexes and lattice methanol molecules into extended 2D supramolecular network (Fig.2b).

However, complex **4** is binuclear, and the asymmetric unit contains a half of the molecule

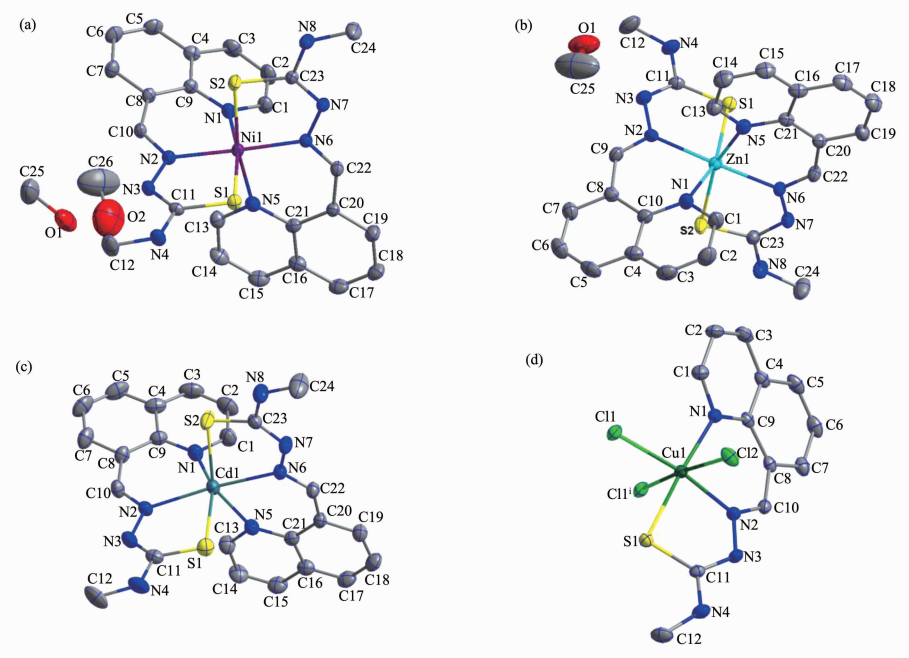

Symmetry codes: [i] $-x+2, -y, -z+2$

Fig.1 Diamond drawing of the asymmetric unit of **1~4** (a~d) with 30% thermal ellipsoids

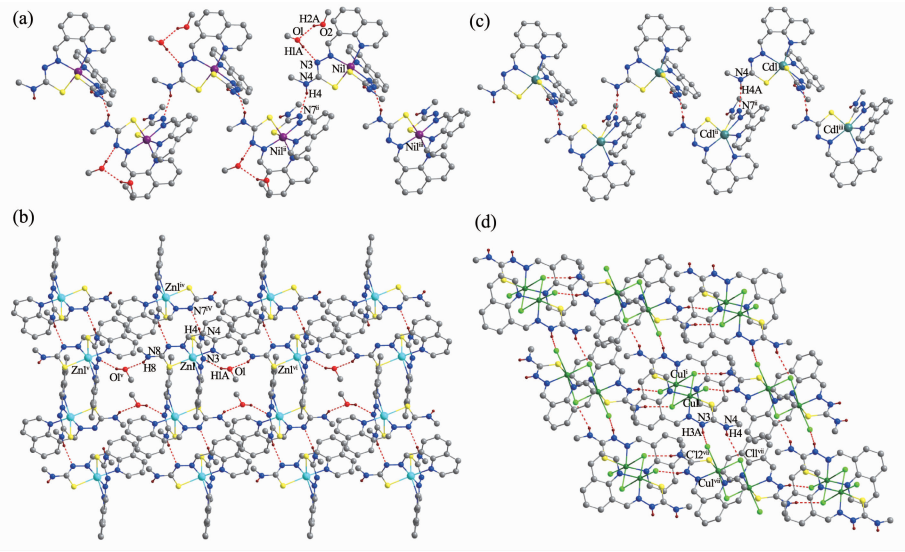

Hydrogen bonds shown in dashed line; H atoms for C-H bonds are omitted for clarity; Symmetry codes: [i] $-x+2,-y, -z+2$; [ii] $-x+1, y+1/2, -z+1/2$; [iii] $-x+1, y-1/2, -z+1/2$; [iv] $-x, y+1/2, -z+1/2$; [v] $x, -y+1/2, z+1/2$; [vi] $x, -y+5/2, z-1/2$; [vii] $-x+1, y-1/2, -z+3/2$

Fig.2 Chain-like structures along b axis formed via hydrogen bonds in complex **1**(a) and **3**(c); Extended 2D supramolecular structure in complex **2**(b) and **4**(d)

(Fig.1d). Each central Cu (Ⅱ) ion of the dimer is surrounded by one independent neutral ligand and three coordinated chloride anions, two of which act as μ^2-bridges, thus giving a distorted octahedron geometry. It should be noted that the bond lengths of Cu1-Cl2 and Cu1-Cl1[i] (Symmetry codes: [i] $-x+2, -y, -z+2$) are 0.284 9(2) and 0.298 9(2) nm, respectively, which are much longer than that of the normal Cu-Cl bond (Cu1-Cl1 0.223 7(2) nm). In the solid state, the intermolecular N-H ⋯ Cl hydrogen bonds are helpful to construct an

Table 2 Selected bond lengths (nm) and angles (°) in complexes 1~4

			1		
Ni1-N1	0.214 5(3)	Ni1-N2	0.205 6(3)	Ni1-N5	0.215 2(3)
Ni1-N6	0.205 0(3)	Ni1-S1	0.238 34(10)	Ni1-S2	0.239 01(11)
N6-Ni1-N2	170.53(10)	N1-Ni1-N5	84.05(10)	N6-Ni1-S2	81.74(8)
N6-Ni1-N1	98.85(10)	N6-Ni1-S1	91.97(8)	N2-Ni1-S2	91.70(8)
N2-Ni1-N1	87.90(10)	N2-Ni1-S1	82.01(8)	N1-Ni1-S2	89.81(8)
N6-Ni1-N5	88.79(10)	N1-Ni1-S1	167.95(8)	N5-Ni1-S2	167.81(8)
N2-Ni1-N5	98.56(11)	N5-Ni1-S1	90.93(8)	S1-Ni1-S2	97.01(4)
			2		
Zn1-N1	0.224 0(4)	Zn1-N2	0.216 0(4)	Zn1-N5	0.225 5(4)
Zn1-N6	0.214 3(3)	Zn1-S1	0.238 88(13)	Zn1-S2	0.240 92(15)
N6-Zn1-N2	171.74(14)	N1-Zn1-N5	80.42(14)	N6-Zn1-S2	79.78(10)
N6-Zn1-N1	104.83(14)	N6-Zn1-S1	93.39(10)	N2-Zn1-S2	96.98(10)
N2-Zn1-N1	82.53(14)	N2-Zn1-S1	80.04(10)	N1-Zn1-S2	87.91(12)
N6-Zn1-N5	84.56(13)	N1-Zn1-S1	159.41(11)	N5-Zn1-S2	157.39(10)
N2-Zn1-N5	100.58(13)	N5-Zn1-S1	92.07(10)	S1-Zn1-S2	104.97(6)
			3		
Cd1-N1	0.240 7(7)	Cd1-N2	0.237 1(6)	Cd1-N5	0.243 7(6)
Cd1-N6	0.235 6(6)	Cd1-S1	0.252 6(2)	Cd1-S2	0.254 3(3)
N6-Cd1-N2	171.2(2)	N1-Cd1-N5	80.3(2)	N6-Cd1-S2	75.63(17)
N6-Cd1-N1	110.7(2)	N6-Cd1-S1	95.43(17)	N2-Cd1-S2	104.77(17)
N2-Cd1-N1	78.1(2)	N2-Cd1-S1	76.16(16)	N1-Cd1-S2	89.4(2)
N6-Cd1-N5	78.5(2)	N1-Cd1-S1	150.00(18)	N5-Cd1-S2	146.60(17)
N2-Cd1-N5	104.0(2)	N5-Cd1-S1	91.24(17)	S1-Cd1-S2	111.80(11)
			4		
Cu1-N1	0.202 2(3)	Cu1-N2	0.194 4(3)	Cu1-S1	0.227 32(19)
Cu1-Cl1	0.223 7(2)	Cu1-Cl2	0.284 9(2)	Cu1-Cl1^{i}	0.298 9(2)
N2-Cu1-N1	90.22(12)	Cl1-Cu1-S1	87.91(6)	N2-Cu1-Cl1^{i}	87.14(9)
N2-Cu1-Cl1	171.67(7)	N2-Cu1-Cl2	86.81(9)	N1-Cu1-Cl1^{i}	84.98(10)
N1-Cu1-Cl1	97.71(9)	N1-Cu1-Cl2	92.33(10)	Cl1-Cu1-Cl1^{i}	90.99(7)
N2-Cu1-S1	83.96(9)	Cl1-Cu1-Cl2	95.38(7)	S1-Cu1-Cl1^{i}	89.48(8)
N1-Cu1-S1	172.16(7)	S1-Cu1-Cl2	92.58(9)	Cl2-Cu1-Cl1^{i}	173.37(3)

Symmetry codes: ^{i} $-x+2, -y, -z+2$

Table 3 Hydrogen bonds information in complexes 1~4

D-H…A	*d*(D-H) / nm	*d*(H…A) / nm	*d*(D…A) / nm	∠D-H…A / (°)
		1		
N(4)-H(4)…N(7)^{ii}	0.086	0.217	0.296 0(4)	153.4
O(1)-H(1A)…N(3)	0.082	0.206	0.287 9(4)	172.6
O(2)-H(2A)…O(1)	0.082	0.216	0.288 3(8)	147.6
		2		

Continued Table 3

N(4)-H(4)···N(7)^{vi}	0.086	0.219	0.301 9(6)	160.7
N(8)-H(8)···O(1)^{v}	0.086	0.223	0.303 3(6)	156.1
O(1)-H(1A)···N(3)	0.082	0.221	0.294 4(7)	149.4
		3		
N(4)-H(4)···N(7)^{ii}	0.086	0.228	0.312 5(4)	169.2
		4		
N(3)-H(3A)···Cl(2)^{vii}	0.086	0.216	0.297 9(3)	160.0
N(4)-H(4)···Cl(1)^{vii}	0.086	0.258	0.325 7(4)	135.9

Symmetry codes: ^{ii} $-x+1, y+1/2, -z+1/2$; ^{iv} $-x, y+1/2, -z+1/2$; ^{v} $x, -y+1/2, z+1/2$; ^{vii} $-x+1, y-1/2, -z+3/2$

extended 2D supramolecular network (Fig.2d).

2.2 IR spectra

The most useful for determining the mode of coordination of the TSC ligand in infrared spectral bands are the ν(N=C), ν(N=C, quinoline) and ν(S=C) vibrations. Such three bonds of the free TSC is found at 1 598, 1 545 and 822 cm^{-1}, while they shifts to lower frequency in complexes **1** ~**4**, clearly indicating the coordination of imine nitrogen, quinoline nitrogen and sulfur atoms [13-14], which is in accordance with the X-ray diffraction analysis result.

2.3 EB-DNA binding study by fluorescence spectrum

It is well known that EB can intercalate nonspecifically into DNA, which causes it to fluoresce strongly. Competitive binding of other drugs to DNA and EB will result in displacement of bound EB and thus decreasing the fluorescence intensity [17]. The effects of the ligand and complexes on the fluorescence spectra of EB-DNA system are presented in Fig.3. The fluorescence intensities of EB bound to ct-DNA at about 600 nm show remarkable decreasing trends with the increasing concentration of the tested compounds, indicating that some EB molecules are released into solution after the exchange with the compounds. The quenching of EB bound to DNA by the compounds is in agreement with the linear Stern-Volmer equation: $I_0/I = 1 + K_{sq}\, r$ [18], where I_0 and I represent the fluorescence intensities in the absence and presence of quencher, respectively, K_{sq} is the

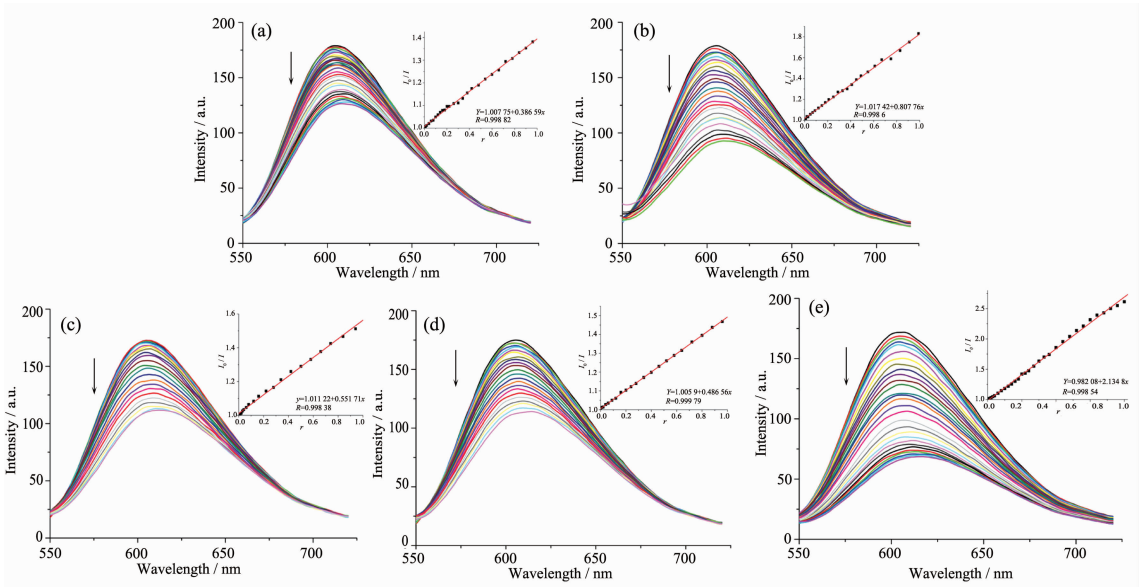

Arrow shows the fluorescence intensities change of EB-DNA system upon increasing tested compound concentration; Inset: plot of I_0/I versus r

Fig.3 Emission spectra of EB-DNA system in the presence of HL (a) and complexes **1**~**4**(b~e), respectively

linear Stern-Volmer quenching constant, r is the ratio of the concentration of quencher and DNA. In the quenching plots of I_0/I versus r, K_{sq} values are given by the slopes. The K_{sq} values are 0.808, 0.552, 0.487 and 2.315 for complexes **1**~**4**, respectively, while that of the ligand HL is tested to be 0.387. The results indicate that interactions of the complexes with DNA are stronger than that of the ligand HL, probably due to the higher rigidity of the complexes, which is in accordance with the literature [14]. In addition, complex 4 has the highest quenching ability among the tested complexes, this could be explained from two aspects: (1) Cu(Ⅱ) plays a significant role in biological systems, and Cu(Ⅱ) complexes usually have higher biological activities than the other transition metal ones[19]; (2) the ligand HL in complex **4** is neutral, and thus the N-H bond at N2 position could act as an additional hydrogen bond donor, making it insert base pairs of DNA more easily than complexes **1**~**3**.

References:

[1] Majid R, Hassan K. *Coord. Chem. Rev*., **2014**,**280**:203-253

[2] Soares M A, Lessa J A, Mendes I C, et al. *Bioorg. Med. Chem*., **2012**,**20**:3396-3409

[3] Qi J, Liang S, Gou Y, et al. *Eur. J. Med. Chem*., **2015**,**96**: 360-368

[4] Li M X, Zhang L Z, Yang M, et al. *Bioorg. Med. Chem. Lett*., **2012**,**22**:2418-2433

[5] Li M X, Zhang L Z, Zhang D, et al. *Eur. J. Med. Chem*., **2011**,**46**:4383-4390

[6] Matesanz A I, Leitao I, Souza P. *J. Inorg. Biochem*., **2013**, **125**:26-31

[7] Matesanz A I, Souza P. *Inorg. Chem. Commun*., **2013**,**27**:5-8

[8] Qi J, Su L, Gou Y, et al. *Eur. J. Med. Chem*., **2015**,**96**:360-368

[9] Jansson P J, Sharpe P C, Bernhardt P V, et al. *J. Med. Chem*., **2010**,**53**:5759-5769

[10]Bacher F, Enyedy E A, Nagy N V, et al. *Inorg. Chem*., **2013**,**52**:8895-8908

[11]Enyedy E A, Primik M F, Kowol C R, et al. *Dalton Trans*., **2011**,**40**:5895-5905

[12]Bourosh P N, Revenko M D, Stratulat E F, et al. *Russ. J. Inorg.Chem*., **2014**,**59**:545-557

[13]Revenko M D, Bourosh P N, Stratulat E F, et al. *Russ. J. Inorg. Chem*., **2010**,**55**:1387-1397

[14]MAO Pan-Dong (毛盼东), YAN Ling-Ling (闫玲玲), WANG Wen-Jing (王文静), et al. *Chinese J. Inorg. Chem.*(无机化学学报), **2016**,**32**:555-561

[15]Sheldrick G M. *SADABS*, University of Göttingen, Germany, **1996**.

[16]Sheldrick G M. *SHELX*-97, *Program for the Solution and the Refinement of Crystal Structures*, University of Göttingen, Germany, **1997**.

[17]Yang Z Y, Wang Y, Wang Y. *Bioorg. Med. Chem. Lett*., **2007**,**17**:2096-2101

[18]SHEN Wei(沈伟), HU Wei-Ji(胡未极), WU Xiao-Yong (吴小勇), et al. *Chinese J. Inorg. Chem.* (无机化学学报), **2016**,**32**:1101-1110

[19]Nath M, Vats M, Roy P. *Eur. J. Med. Chem*., **2013**,**59**:310-321